Negative Volume Thermal Expansion Via Orbital and Magnetic Orders in $Ca_2Ru_{1-x}Cr_xO_4$ ($0 < x < 0.13$)

T. F. Qi,[1,2] O. B. Korneta,[1,2] S. Parkin,[1,3] L. E. De Long,[1,2] P. Schlottmann,[4] and G. Cao[1,2,*]

[1]*Center for Advanced Materials, University of Kentucky, Lexington, Kentucky 40506, USA*
[2]*Department of Physics and Astronomy, University of Kentucky, Lexington, Kentucky 40506, USA*
[3]*Department of Chemistry, University of Kentucky, Lexington, Kentucky 40506, USA*
[4]*Department of Physics, Florida State University, Tallahassee, Florida 32306, USA*

(Received 30 July 2010; published 22 October 2010)

Ca_2RuO_4 undergoes a metal-insulator transition at $T_{MI} = 357$ K, followed by a well-separated transition to antiferromagnetic order at $T_N = 110$ K. Dilute Cr doping for Ru reduces the temperature of the orthorhombic distortion at T_{MI} and induces ferromagnetic behavior at T_C. The lattice volume V of $Ca_2Ru_{1-x}Cr_xO_4$ ($0 < x < 0.13$) abruptly expands with cooling at both T_{MI} and T_C, giving rise to a total volume expansion $\Delta V/V \approx 1\%$, which sharply contrasts the smooth temperature dependence of the few known examples of negative volume thermal expansion driven by anharmonic phonon modes. In addition, the near absence of volume thermal expansion between T_C and T_{MI} represents an Invar effect. The two phase transitions, which surprisingly mimic the classic freezing transition of water, suggest an exotic ground state driven by an extraordinary coupling between spin, orbit, and lattice degrees of freedom.

DOI: 10.1103/PhysRevLett.105.177203 PACS numbers: 75.25.Dk, 65.40.De, 71.30.+h, 75.10.Nr

The layered 4*d*-transition metal oxides have attracted increasing interest since the comparable magnitudes of their intra-atomic Coulomb interaction U and 4*d*-bandwidth W can leave them precariously balanced on the border between metallic and insulating behavior, or on the verge of long-range magnetic order. Therefore, moderately strong spin-orbit interactions, as well as weaker perturbations such as slight changes in lattice parameters, can induce drastic changes in the character of their electronic ground states. This is dramatically illustrated by Sr_2RuO_4 and Ca_2RuO_4, where the prototypical *p*-wave superconducting state [1] of the former compound strongly contrasts with the more distorted structure (due to the smaller ionic radius $r_{Ca} < r_{Sr}$) and first-order metal-insulator (MI) transition observed for the latter [2,3].

Extensive investigations of Ca_2RuO_4 [4,5] have established that a strong cooperative Jahn-Teller distortion removes the degeneracy of the three Ru t_{2g} orbitals (d_{xy}, d_{yz}, d_{zx}) via a transition to orbital order that, in turn, drives the MI transition at $T_{MI} = 357$ K [6–12]. Classic Mott insulators undergo simultaneous transitions to antiferromagnetic (AFM) order and an insulating state at T_{MI}. However, Ca_2RuO_4 undergoes AFM order at $T_N = 110$ K $\ll T_{MI}$ [2], and is therefore a highly interesting and unique archetype of a MI transition that is strongly coupled to a structural transition that is not driven by AFM exchange interactions.

The MI transition of Ca_2RuO_4 is signaled by an abrupt jump in electrical resistivity $\rho(T)$ accompanying a structural transition from a high-T tetragonal to low-T orthorhombic, which culminates in a striking increase of $\rho(T)$ by over 9 orders of magnitude between T_{MI} and 70 K [2,3], as shown in Fig. 1(a). Although the a axis of Ca_2RuO_4 contracts by 1.5% below T_{MI}, the b axis expands by 3%; the combined effect of these conflicting uniaxial thermal expansions drives a particularly severe orthorhombic distortion of the tetragonal basal plane which shatters single-crystal samples and strongly contracts the lattice volume by 1.3% as T is lowered from 400 K to 70 K [3].

Although controversy over the exact nature of the orbital ground state remains [8–12], the extraordinary sensitivity of T_{MI} and electrical resistivity to the application of modest pressure [8] or very slight changes in lattice parameters [6,7] clearly indicate that the lattice drives the highly unusual behavior of Ca_2RuO_4. On the other hand, Cr substitution for Ru in layered ruthenates generally results in no structural change, but does induce interesting magnetic behavior [as demonstrated by $SrRu_{1-x}Cr_xO_3$ [13–15], $CaRu_{1-x}Cr_xO_3$ [16], and $Ca_3(Ru_{1-x}Cr_x)_2O_7$ [17]], which led us to pursue Cr substitution as an effective tool to investigate the curious dominance of lattice over magnetic degrees of freedom in Ca_2RuO_4.

Herein, we report the surprising finding that very dilute Cr doping for Ru in Ca_2RuO_4 not only induces spin canting and ferromagnetic (FM) behavior at a lower transition T_C (which extrapolates to T_N for $x = 0$), it strongly reduces the structural distortion and depresses T_{MI}. More important, the lattice volume V of $Ca_2Ru_{1-x}Cr_xO_4$ ($0 < x < 0.12$) abruptly expands with cooling just below T_{MI} and, subsequently, just below T_C, giving rise to a large net volume expansion $\Delta V/V \approx 1\%$ as temperature decreases over the range $90 < T \leq 295$ K. The negative volume thermal expansion (NVTE) we observe in $Ca_2Ru_{1-x}Cr_xO_4$ is extraordinary, because: (1) It is a large, bulk elastic anomaly affected by only a few percent Cr substitution. (2) NVTE is generally smoothly varying with temperature, found only in a handful of materials where it is attributed to highly

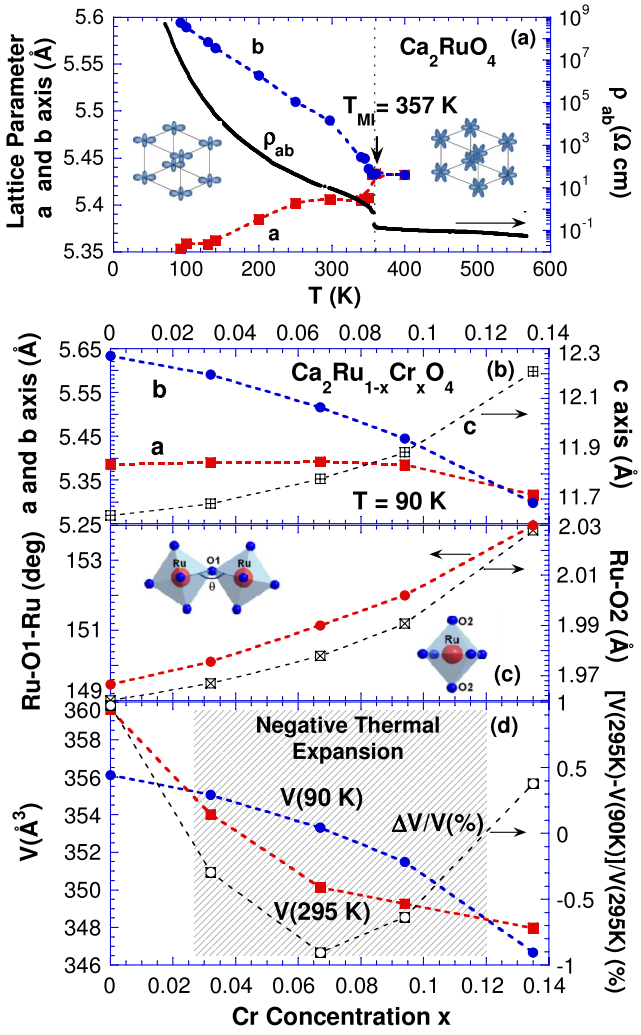

FIG. 1 (color online). (a) Temperature dependence of the a and b axis lattice parameters, and the ab-plane resistivity ρ_{ab} (right scale) for $x = 0$. Inset: Schematics of orbital order and disorder. (b) Cr concentration (x) dependence of the a, b and c axis lattice parameters (right scale) for $T = 90$ K. (c) Ru-O1-Ru bond angle and the Ru-O2 bond distance (right scale) for $T = 90$ K. Inset: Schematics of the distorted Ru-O1-Ru bond angle θ and a RuO_6 octahedron. (d) Unit cell volume V for $T = 90$ K and 295 K, and thermal expansion ratio $[V(295\ \mathrm{K}) - V(90\ \mathrm{K})]/V(295\ \mathrm{K})$ (right scale) for $0 \leq x \leq 0.135$.

anharmonic vibrational modes [18–21]. In contrast, the "two-step" NVTE we observe for $Ca_2Ru_{1-x}Cr_xO_4$ arises from consecutive, discrete transitions to orbital and magnetic order, a phenomenon never found before. (3) Nearly zero volume thermal expansion is observed over the wide (100 K) interval spanning T_C and T_{MI}, which constitutes a strong "Invar effect."

Single crystals of $Ca_2Ru_{1-x}Cr_xO_4$ with $0 < x < 0.135$ were grown using a floating zone optical furnace; technical details are described elsewhere [22]. The structures of single-crystal $Ca_2Ru_{1-x}Cr_xO_4$ samples were refined at various temperatures between 90 and 295 K using a Nonius-Kappa CCD single-crystal x-ray diffractometer (XRD) with sample temperature set using a nitrogen stream. Structures were refined by full-matrix least-squares using the SHELX-97 programs [22,23]. All structures were strongly affected by absorption and extinction, and the data were corrected for anisotropic absorption by comparison of symmetry-equivalent reflections using the program SADABS [24]. Detailed structural results and analysis will be published elsewhere [22]. The Cr concentration x was determined by energy dispersive x-ray (EDX) analysis. Measurements of magnetization $M(T, H)$ and electrical resistivity $\rho(T)$ for $T < 400$ K were performed using either a quantum design physical property measurement system or magnetic property measurement system. All measurements [XRD, EDX, $M(T, H)$, and $\rho(T)$] were performed on the same single crystal for each composition x to ensure consistency (single-crystal XRD requires a small piece taken from each single crystal studied).

Figure 1 illustrates some overall trends observed in our structural data for $Ca_2Ru_{1-x}Cr_xO_4$ ($0 < x < 0.135$) single crystals. Although Cr doping generally preserves the low-T orthorhombic symmetry ($Pbca$), it reduces and eventually suppresses the orthorhombic distortion [e.g., $(b - a) = 0.247$ Å for $x = 0$, but $(b - a) = 0.018$ Å for $x = 0.135$ at $T = 90$ K; see Fig. 1(b)] [22]. The weakening structural distortion is accompanied by relaxation of the Ru-O1-Ru bond angle θ and elongation of the RuO_6 octahedra (i.e., the Ru-O2 bond distance), as shown in Fig. 1(c). More important, Cr doping causes the unit cell volume V to expand as T is lowered from 295 K to 90 K for $0.032 \leq x < 0.13$, as shown in Fig. 1(d).

The first-order MI transition T_{MI} is definitively marked by a jump in the basal plane resistivity ρ_{ab}, as shown in Fig. 2(a); T_{MI} also drops rapidly with increasing x, which we will show is closely related to the structural relaxation. Remarkably, the first-order transition at T_{MI} is suppressed to zero at a critical composition $x_{cr} = 0.135$, simultaneous with both the disappearance of the orthorhombic distortion [see Fig. 1(b)], and the return of the thermal expansion $\Delta V/V$ to normal behavior [see Fig. 1(d)]. The onsets of orbital order and NVTE are slightly different chiefly because of a strong hysteresis effect due to the first-order transition [22]. Clearly, the anomalous NVTE is strongly coupled to the onset of orbital ordering.

The stability of the AFM state is also critically dependent upon both the Ru-O1-Ru bond angle θ and a concomitant elongation of the apical Ru-O2 distance, which undergo similar, finite shifts at only modest Cr doping levels [Fig. 1(c)]. In particular, the magnetic critical temperature $T_C(x)$ slowly increases and peaks at 130 K near $x = 0.067$. Moreover, the positive Curie-Weiss temperature θ_{CW} estimated from high-T fits of magnetic data increases with x, indicating an increasing FM character of the volume-averaged exchange interaction [see Fig. 2(b), inset]. Given the low saturation moment ($\sim 0.04\mu_B$/f.u. for $x = 0.032$) and the strong magnetic field dependence of $M(H)$ shown in Fig. 2(c), the FM behavior is likely a result of spin canting in an otherwise collinear AFM spin arrangement. The T_C peak

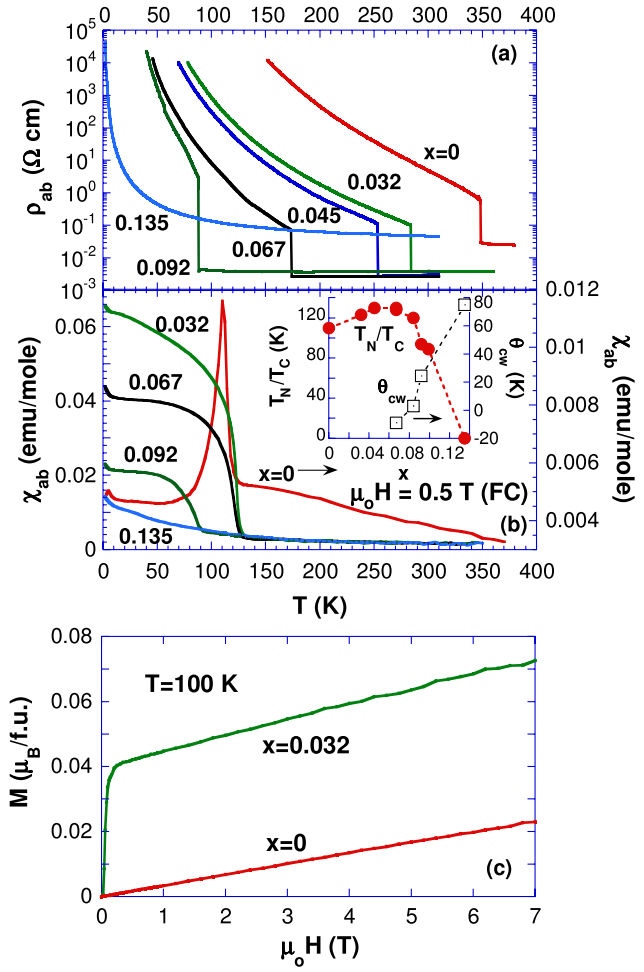

FIG. 2 (color online). Temperature dependences of (a) the ab-plane resistivity ρ_{ab}, (b) the magnetic susceptibility χ_{ab} at applied field $\mu_0 H = 0.5$ T for $0 \leq x \leq 0.135$, and (c) the isothermal magnetization $M(H)$ at 100 K for representative compositions $x = 0$ and 0.032. Inset: T_N, T_C and Curie-Weiss temperature θ_{CW} vs x.

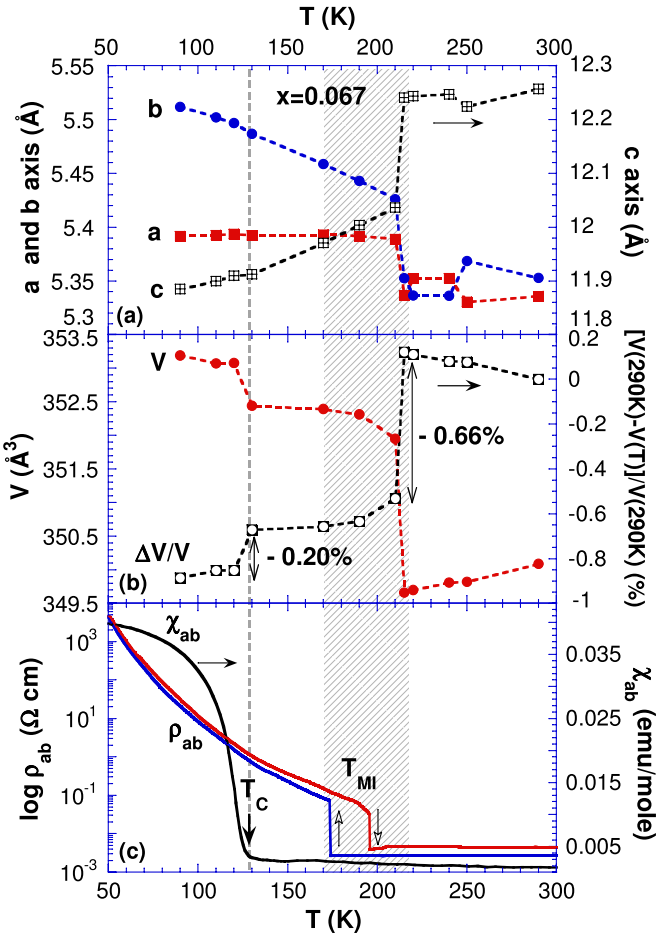

FIG. 3 (color online). For $x = 0.067$, temperature dependences of: (a) lattice parameters a, b and c axis (right scale), (b) unit cell volume V and thermal expansion ratio $\Delta V/V$ (right scale), and (c) ab-plane resistivity ρ_{ab} and magnetic susceptibility χ_{ab} at $\mu_0 H = 0.5$ T. The shaded area indicates a region where the structural phase transition and first-order MI transition occur.

is followed by a suppression of magnetic order near the critical composition $x_{cr} = 0.135$ [shown in Fig. 2(b)], simultaneous with the suppressions of orbital order and NVTE.

The close correlation of NVTE with orbital and magnetic order is documented by data for a representative composition $x = 0.067$ [see Fig. 3)], which illustrates the central findings of this work: (1) Strong, negative linear expansion occurs not only along the b axis, but also along the a axis for $x > 0$ [Fig. 3(a)], which gives rise to the much rarer case of NVTE [25]. (2) Discontinuities in the a , b and c axis lattice parameters signal a first-order phase transition from a high-T tetragonal, to a low-T orthorhombic phase at 210 K [Fig. 3(a)]. (3) V abruptly expands by ~0.66% with decreasing T near 210 K, and expands again by ~0.2% at $T_c = 130$ K, but changes only slightly between these two temperatures [Figs. 3(b) and 3(c)].

The extraordinary, strong dependence of the structural, magnetic, and electrical properties of $Ca_2Ru_{1-x}Cr_xO_4$ on Cr content can be explained as follows. The drastic decrease in T_{MI} observed with increasing Cr doping in $Ca_2Ru_{1-x}Cr_xO_4$ closely tracks the rapidly weakening orthorhombicity, as well as the reduced tilt and elongation of RuO_6 octahedra [Figs. 1(b) and 1(c)], as x increases, and the eventual disappearance of T_{MI} is concomitant with vanishing orthorhombicity for $x_{cr} = 0.135$ [Fig. 2(a)]. Indeed, it is predicted that the orbital ground state is governed by d_{xy} ferro-orbital order that is stabilized by the Jahn-Teller distortion [12]; Cr doping readily weakens and eventually removes the Jahn-Teller distortion, thus the existence of d_{xy} orbital order and T_{MI}. Moreover, the increasing Ru-O2 bond distance and Ru-O1-Ru bond angle [Fig. 1(c)] destabilize the collinear AFM state [26], which, in turn, lead to weak FM behavior and spin canting. A competition between AFM and FM couplings persists to $x < 0.135$, but Tc decreases rapidly as x increases above 0.06 [Fig. 2(b)]. The fact that NVTE does not occur for $x = 0$ underscores how Cr doping softens the lattice and "unlocks" strongly buckled RuO_6 octahedra [22], allowing both the a and b axis to expand while preserving

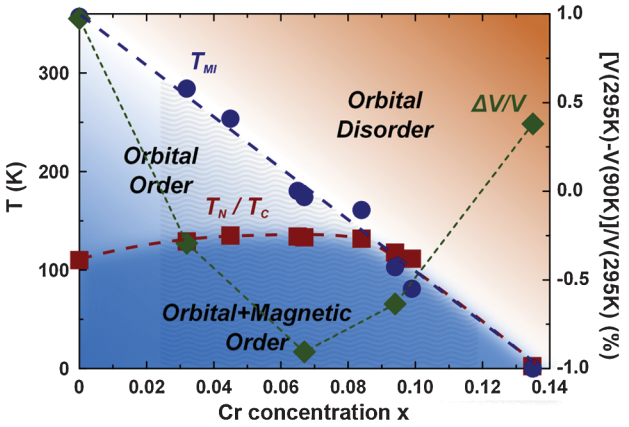

FIG. 4 (color). The T-x phase diagram summarizing observed phase transitions and phase types. Right scale shows the Cr concentration (x) dependence of the thermal expansion ratio $\Delta V/V$. Note that the hatched region represents negative volume thermal expansion.

the structural symmetry. Consequently, V abruptly expands on cooling just below T_{MI}, where orbital ordering occurs, and further expands at T_C. Cr doping also relaxes the orthorhombic distortion that, via a highly unusual spin-lattice coupling, weakens the AFM state, and results in an extraordinary increase in volume on cooling.

The principal conclusion we draw from our observations [Fig. 3] is that the unique NVTE anomalies in $Ca_2Ru_{1-x}Cr_xO_4$ are directly associated with the onsets of orbital ordering at T_{MI}, and magnetic ordering at T_C, and between T_{MI} and T_C, V remains essentially constant, an Invar effect (e.g., the slight or nearly zero thermal expansion first observed in certain Ni-Fe alloys [27]). This behavior surprisingly mimics the classic example of NVTE observed at the freezing point of water. A phase diagram given in Fig. 4 shows that the first-order (T_{MI}) and second-order (T_C) transition lines separate three states that meet at a tricritical point. The coexisting orbital and magnetic orders "melt" when both T_{MI} and T_C disappear near $x = 0.12 \pm 0.01 \approx x_{\mathrm{cr}}$, implying that x is a critical Cr concentration.

NVTE is seen in only a handful of materials such as ZrW_2O_8 and $ZnCr_2Se_4$, where it is primarily associated with transverse thermal motion of oxygen or highly anharmonic vibrational modes [17–20]; the latter effect is related to spin canting and a spin-lattice coupling at low temperatures [21], but in these cases, no anomalies in other physical properties (e.g., a MI transition) are observed. In contrast, the unusual "two-step" temperature dependence of V and the simultaneous suppressions of magnetic and orbital order and orthorhombic distortion with dilute Cr doping indicate the existence of a novel coupling between spin, orbital, and lattice degrees of freedom in $Ca_2Ru_{1-x}Cr_xO_4$.

The conspicuously wide separation between T_{MI}, on the one hand, and T_N or T_C on the other, for the pure ($x = 0$) and more dilute Cr-doped samples poses the surprising possibility that spin-orbit coupling has a more subtle influence on the physical properties of $Ca_2Ru_{1-x}Cr_xO_4$ than is commonly anticipated for other ruthenates [7,8]. The nearly constant V observed between T_{MI} and T_C is a new manifestation of the technologically important Invar effect, and reinforces the conclusion that the strong NVTE in $Ca_2Ru_{1-x}Cr_xO_4$ is closely coupled to the onsets of orbital and magnetic order.

The negative volume thermal expansion via orbital and magnetic orders found in $Ca_2Ru_{1-x}Cr_xO_4$ suggests an exotic ground state, as well as a paradigm for functional materials with highly unusual thermal expansion and electronic characteristics.

This work was supported by NSF through Grants No. DMR-0552267, No. DMR-0856234 (G. C), and No. EPS-0814194 (G. C, L. E. D), and by DoE through Grants No. DE-FG02-97ER45653 (L. E. D) and No. DE-FG02-98ER45707 (P. S.).

*Corresponding author: cao@uky.edu

[1] Y. Maeno *et al.*, Nature (London) **372**, 532 (1994).
[2] G. Cao *et al.*, Phys. Rev. B **56**, R2916 (1997).
[3] C. S. Alexander *et al.*, Phys. Rev. B **60**, R8422 (1999).
[4] M. Braden *et al.*, Phys. Rev. B **58**, 847 (1998).
[5] M. A. Carpenter and C. J. Howard, Acta Crystallogr. Sect. B **65**, 134 (2009).
[6] G. Cao *et al.*, Phys. Rev. B **61**, R5053 (2000).
[7] S. Nakatsuji, and Y. Maeno, Phys. Rev. Lett. **84**, 2666 (2000).
[8] C. S. Snow *et al.*, Phys. Rev. Lett. **89**, 226401 (2002).
[9] T. Hotta and E. Dagotto, Phys. Rev. Lett. **88**, 077202 (2002).
[10] T. Mizokawa *et al.*, Phys. Rev. Lett. **87**, 077202 (2001).
[11] J. S. Lee *et al.*, Phys. Rev. Lett. **89**, 257402 (2002).
[12] J. H. Jung *et al.*, Phys. Rev. Lett. **91**, 056403 (2003).
[13] L. Pi *et al.*, J. Phys. Condens. Matter **14**, 7391 (2002).
[14] B. Dabrowski *et al.*, Phys. Rev. B **70**, 014423 (2004).
[15] Z. H. Han *et al.*, J. Phys. Condens. Matter **17**, 1193 (2005).
[16] V. Durairaj *et al.*, Phys. Rev. B **73**, 214414 (2006).
[17] G. Cao *et al.*, Phys. Rev. Lett. **100**, 016604 (2008).
[18] C. Martineck and F. A. Hummel, J. Am. Ceram. Soc. **51**, 227 (1968).
[19] T. A. Mary *et al.*, Science **272**, 90 (1996).
[20] G. Ernst *et al.*, Nature (London) **396**, 147 (1998).
[21] J. Hemberger *et al.*, Phys. Rev. Lett. **98**, 147203 (2007).
[22] T. F. Qi, S. Parkin, and G. Cao (to be published).
[23] G. M. Sheldrick, Acta Crystallogr. Sect. A **64**, 112 (2008).
[24] G. M. Sheldrick, *SADABS* (University of Göttingen, Germany, 1996).
[25] In order to showcase the convergence of the a and b axis lengths, Fig. 3(a) was drawn without the factor of $\sqrt{2}$ and without having constrained the a and b axis to be equal for the tetragonal phase. Thus, Fig. 3(a) shows that the experimental diffraction data indicate a convergence of the a and b axis at $T > T_{\mathrm{MI}}$.
[26] Z. Fang and K. Terakura, Phys. Rev. B **64**, 020509 (2001).
[27] Mark van Schilfgaarde, I. A. Abrikosov, and B. Johansson, Nature (London) **400**, 46 (1999).